

RSC Advances



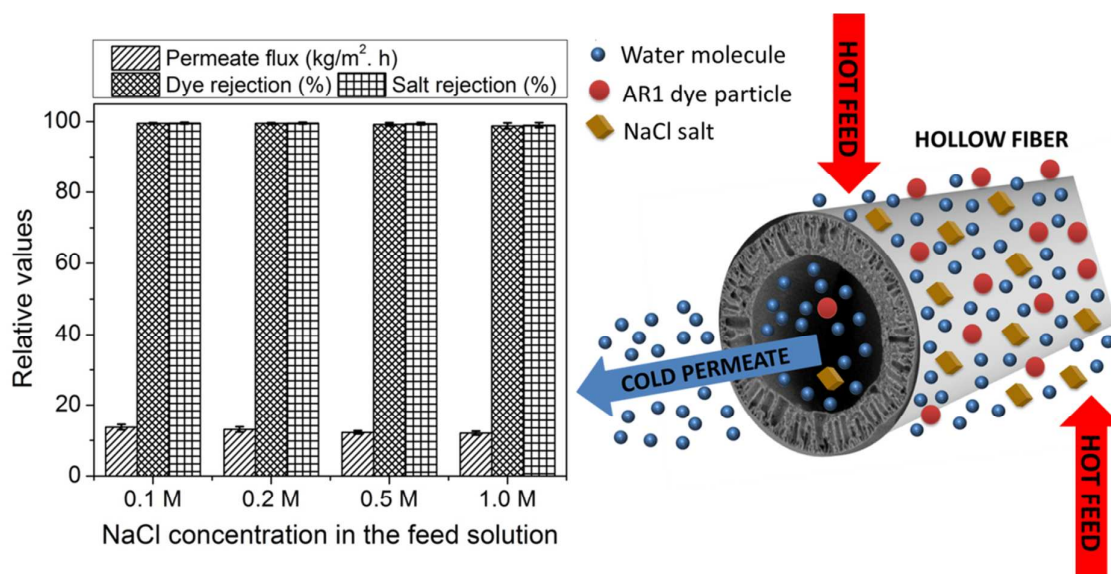
This is an *Accepted Manuscript*, which has been through the Royal Society of Chemistry peer review process and has been accepted for publication.

Accepted Manuscripts are published online shortly after acceptance, before technical editing, formatting and proof reading. Using this free service, authors can make their results available to the community, in citable form, before we publish the edited article. This *Accepted Manuscript* will be replaced by the edited, formatted and paginated article as soon as this is available.

You can find more information about *Accepted Manuscripts* in the [Information for Authors](#).

Please note that technical editing may introduce minor changes to the text and/or graphics, which may alter content. The journal's standard [Terms & Conditions](#) and the [Ethical guidelines](#) still apply. In no event shall the Royal Society of Chemistry be held responsible for any errors or omissions in this *Accepted Manuscript* or any consequences arising from the use of any information it contains.

Graphical abstract



Performances of novel PVDF-Cloisite 15A hollow fiber composite membrane in treating dyeing solution containing 50 ppm AR1 and 0.1–1.0 M NaCl

1 **Performance evaluation of novel PVDF-Cloisite 15A hollow fiber composite membranes**
2 **for treatment of effluents containing dyes and salts using membrane distillation**

3
4
5
6
7 N. M. Mokhtar^a, W.J. Lau^{a,*}, A.F. Ismail^a, W. Youravong^b, W. Khongnakorn^b, K.
8 Lertwittayanon^b
9

10
11
12
13 ^aAdvanced Membrane Technology Research Centre (AMTEC), Universiti Teknologi
14 Malaysia, 81310 Skudai, Johor, Malaysia.

15 ^bMembrane Science and Technology Research Centre (MSTRC), Prince of Songkla
16 University, 90112 Hat Yai, Songkla, Thailand.
17
18
19
20
21
22
23
24
25
26
27
28
29
30

31 *Corresponding author: Tel.: +60 75535926

32 Email address: lwoeijye@utm.my; lau_woeijye@yahoo.com; lau.woeijye09@gmail.com

33 (W.J. Lau)

34 **Abstract**

35

36 The present study reports the performance of novel PVDF-Cloisite 15A hollow fiber
37 composite membrane for the treatment of effluents containing dyes and salts through direct
38 contact membrane distillation (DCMD) process. The performance of the membrane was
39 evaluated by varying several important parameters during DCMD process which included
40 feed properties (type of dyes, dye and salt concentration) and process conditions (feed
41 temperature and flow rate). Experimental results showed that the in-house made membrane
42 was able to achieve stable fluxes and excellent dye rejections (>97%) when tested with feed
43 solutions containing dyes of different classes and molecular weights (MW), except crystal
44 violet (CV) dye. The lower rejection resulted from CV-contained feed is likely due to its
45 small MW coupled with high diffusion rate in aqueous solution. With respect to feed
46 concentration, it is found that an increase in salt concentration in the feed solution had
47 negligible effect on the membrane separation performance. Increasing dye concentration in
48 the feed however led to lower membrane water flux owing to the deposition of dye particles
49 on membrane surface which resulted in severe fouling. Meanwhile, increasing feed
50 temperature and its flow rate could improve membrane flux without affecting the permeate
51 quality. When tested using dyeing solution containing 50 ppm acid red and 1.0 M NaCl, the
52 membrane flux was reported to enhance by 200% and 25% with increasing feed temperature
53 from 50 to 90°C and flow rate from 0.010 to 0.023 m/s, respectively.

54

55

56

57

58

59

60

61

62

63

64

65

66 *Keywords:* membrane distillation; composite membrane; textile wastewater; dye-salt
67 mixtures; membrane fouling

68 1 Introduction

69

70 Wastewater treatment has been a challenge to the textile and dyestuff manufacturing
71 industries due to the color exhibited by the effluents. Colored textile effluents usually
72 represent severe environmental problems as they contain a mixture of chemicals, auxiliaries
73 and dyestuffs of different classes and chemical constitutions with elevated organic and
74 inorganic parameters [1–3]. The colored textile effluents often come from printing and
75 dyeing processes that use high concentrations of dyes, additives and salts to produce high
76 quality fabrics [4]. Synthetic dyes, which are the most common among all other dyes, are
77 typically used in textile industries. They are generally derived from coal tar and petroleum
78 based intermediates [5,6]. According to Sen and Demirer [6], more than 7×10^7 tons of
79 synthetic dyes are produced and consumed worldwide annually. Of these synthetic dyes, azo
80 dyes are the largest and the most common group of dyes used in textile industry [1,7].
81 However, it must be noted that azo dyes are highly toxic, mutagenic and carcinogenic in
82 nature [8]. The presence of a small quantity (even at 1 ppm level) of azo dyes in water can be
83 visible and results in acute effect to the aquatic system due to their high level of toxicity
84 [2,9].

85

86 Owing to ecological factors, a new global trend on developing various sustainable
87 technologies for removal of such colored agents from aqueous solutions is of significant
88 environmental and technical importance. The technologies that have been employed for
89 textile effluent treatment can be categorized based on chemical, physical and biological
90 methods [10–12]. Some of the examples of physical-chemical treatment methods are
91 membrane filtration, coagulation/flocculation, precipitation, flotation, adsorption, ion
92 exchange, electrolysis, advanced oxidation and chemical reduction. With respect to biological
93 methods, bacterial/fungal biosorption and biodegradation in aerobic, anaerobic, anoxic or
94 combined aerobic/anaerobic conditions have been generally reported [10]. Although
95 physical-chemical methods are a good option regarding high color and suspended substances
96 removal, they are associated with some problems such as sludge generation, low chemical
97 oxygen demand (COD) removal and high operating cost. Biological treatment process on the
98 other hand experiences several technical challenges such as difficulty of maintaining bacterial
99 growth, longer period of treatment cycle, etc [13].

100

101 To date, the importance of membrane technologies in textile wastewater treatment is
102 continuously growing. Membrane separation processes have become the best alternative
103 methods that can be adopted for large-scale treatment process owing to the advantages such
104 as environmentally friendly, high removal efficiency, modest energy requirement, etc [14].
105 Among the membrane-based processes, membrane distillation (MD) has been seen as a
106 potential candidate in treating textile effluents as this membrane process can be operated at
107 very low pressure, thus minimizes fouling effect [15–23]. Furthermore, MD can exploit the
108 free energy given by hot effluent discharged by textile industry [16,23]. In order to
109 consistently maintain the effluent temperature during treatment process, low-grade waste
110 and/or alternative energy sources such as solar and geothermal energy can be potentially
111 integrated with MD process [24]. Another promising feature of MD is its ability to reject
112 100% (theoretically) ions, macromolecules, colloids, cells, and other non-volatile organic
113 compounds from the wastewater as its separation mechanism is mainly governed by vapor-
114 liquid equilibrium (VLE) [25].

115

116 In our previous work [21], we have investigated the effect of Cloisite 15A clay
117 loadings (zero–10 wt%) on the properties of polyvinylidene-fluoride (PVDF)-based hollow
118 fiber membranes for MD application. Of the PVDF-Cloisite 15A composite membranes
119 studied, it is found that the incorporation of 3 wt% Cloisite 15A was the ideal loading to
120 produce best performing composite membrane by taking into consideration the membrane
121 structural properties and separation characteristics. In this work, we will further evaluate the
122 potential of this membrane in treating feed solutions containing dyes and salts via direct
123 contact membrane distillation (DCMD) system. The separation performances of this
124 membrane will be studied under different conditions by varying the properties of feed
125 solution as well as process conditions.

126

127 **2 Experimental**

128 **2.1 Materials**

129

130 Five synthetic dyes supplied by Sigma-Aldrich were used as received and their
131 classification and chemical structure are shown in Figure 1 and Table 1, respectively. Salt,
132 sodium chloride (NaCl, MW = 58.44 g/mol) supplied by Merck was added to the dyeing
133 solution to simulate industrial textile wastewater which often contains dissolved salts in the
134 effluent.

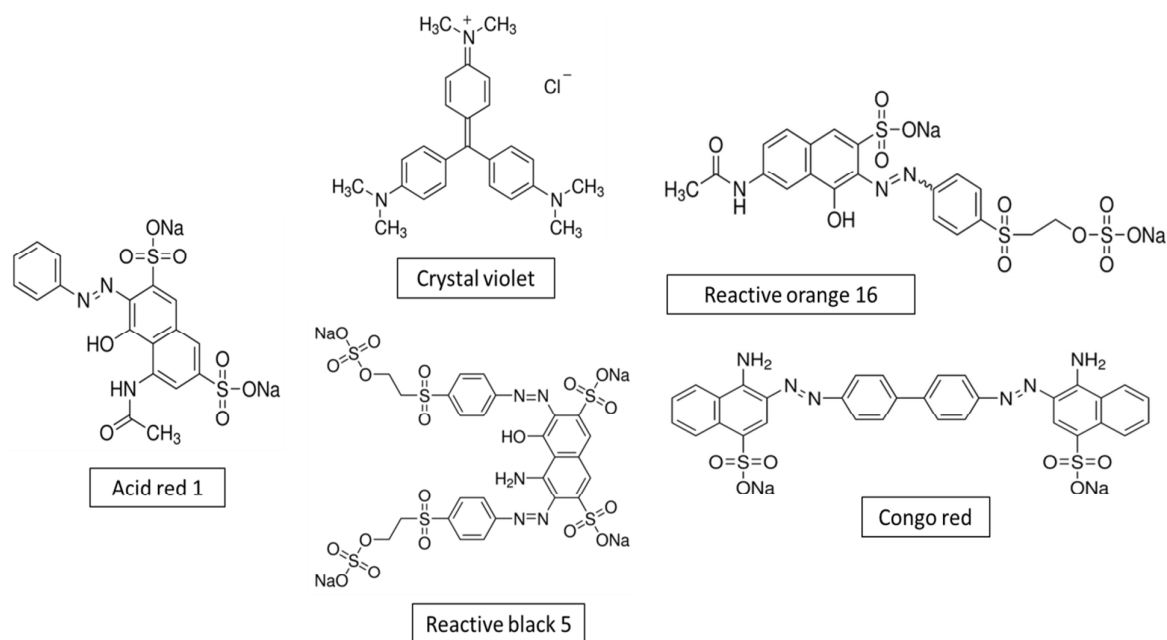
135

Table 1 Overview of dye classification used in this study [1,26]

Class	Principal substrates	Method of application	Chemical types	Dye fixation (%)	Dyes used in this study
Acid	Nylon, wool, silk, inks, leather	Usually from neutral to acidic dyebaths	Azo (including premetallized), anthraquinone, triphenylmethane, azine, xanthene, nitro and nitroso	89-95	Acid red 1 (AR1), Congo red (CR)
Basic	Polyacrylonitrile, modified nylon, polyester, inks	Applied from acidic dyebaths	Cyanine, hemicyanine, diazahemicyanine, diphenylmethane, triarylmethane, azo, azine, xanthene, acridine, oxazine, anthraquinone	95-100	Crystal violet (CV)
Reactive	Cotton, wool, silk, nylon	Reactive site on dye reacts with functional group on fiber to bind dye covalently under influence of heat and pH (alkaline)	Azo, anthraquinone, phthalocyanine, formazan, oxazine, basic	50-90	Reactive orange 16 (RO16), Reactive black 5 (RB5)

136

137



138

139

Figure 1 Chemical structure of the synthetic dyes used in this work

140 2.2 Stokes diameter of dye particle

141

142 The diameter, d_A (nm) of the dye particle was measured using Stokes-Einstein
143 equation [27]:

144

$$145 \quad d_A = \frac{kT}{3\pi \mu_B D_{AB}} \quad (3)$$

146

147 where k is the Boltzmann coefficient (J/K), T is temperature (K), μ_B is the water viscosity
148 (Pa.s) and D_{AB} is the diffusion coefficient (m²/s) of dye in water. The D_{AB} can be further
149 defined according to the Wilke-Chang equation:

150

$$151 \quad D_{AB} = 1.173 \times 10^{-16} \sqrt{\phi M_B} \frac{T}{\mu_B V_A^{0.6}} \quad (4)$$

152

153 where ϕ is the water association parameter, M_B is the MW of water (g/mol), μ_B is the water
154 viscosity (Pa.s) and V_A is the molar volume of dye particle (m³/kg.mol). The molar volume
155 for each dye was calculated using a group contribution method [28].

156

157 2.3 Membrane fabrication

158

159 PVDF-Cloisite 15A dope solution consisted of 12 wt% PVDF and 3 wt% Cloisite
160 15A (i.e. clay concentration was determined based on the total weight of PVDF) was
161 prepared by dissolving the PVDF pellets and clay powder in the NMP (80 wt%) and EG (8
162 wt%) mixture, while stirring at 60°C, until the solution became homogeneous. After that, the
163 PVDF-Cloisite 15A hollow fiber composite membrane was fabricated using dry-jet wet
164 spinning technique in which the detailed fabrication procedure can be found in our previously
165 published work [21]. After air-drying process, the membrane was subject to several
166 characterizations to determine its structural properties.

167

168 2.4 Direct contact membrane distillation (DCMD) experiments

169

170 A stainless steel module containing PVDF-Cloisite 15A hollow fiber composite
171 membrane was prepared and used to determine the performances of the membranes during

172 DCMD process. Table 2 shows the details of the membrane properties and its module. The
173 DCMD system that was used in this work is illustrated in Figure 2, together with SEM
174 images of the hollow fiber composite membrane. The system was designed to have two
175 circulating streams, i.e. hot stream also known as feed stream (circulated through the
176 membrane shell-side) and cold stream (fed through the lumen-side of the hollow fiber
177 membrane). Both solution temperatures were controlled using coiled heater (830,
178 PROTECH) and chiller (F26-ED, JULABO), respectively. The change of feed concentration
179 in the feed tank during experiment was assumed to be negligible as large feed volume (5 L)
180 was used. In order to avoid membrane flux decline caused by dye deposition (fouling), a new
181 membrane module was used whenever there was a change in the feed property and/or process
182 condition.

183

184 Prior to the dyeing solution treatment process, the permeate flux, J_v of membrane
185 ($\text{kg}/\text{m}^2\cdot\text{h}$) was determined using Eq. 1.

186

$$187 \quad J_v = \frac{\Delta W}{A\Delta t} \quad (1)$$

188

189 where ΔW (kg) is the weight of permeate collected over a predetermined time Δt (h) of
190 process and A (m^2) is the effective membrane area. To determine the solute (dye or salt)
191 rejection, R (%) of the membrane, Eq. 2 was employed.

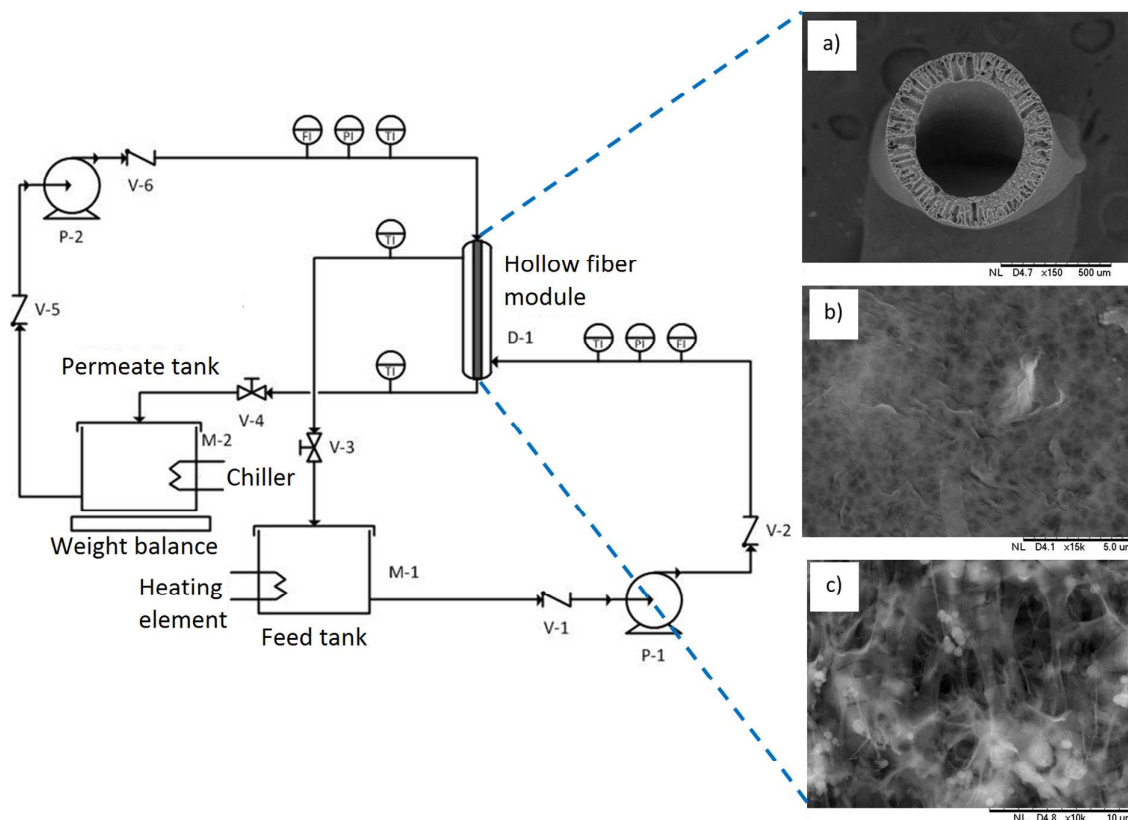
192

$$193 \quad R = \left(1 - \frac{C_p}{C_f} \right) \times 100 \quad (2)$$

194

195 where C_p and C_f stand for permeate and feed concentration (mg/L), respectively. The results
196 of flux and rejection reported in this work were the average of three measurements.

197



198

199 **Figure 2** Schematic DCMD experimental setup and the SEM micrographs of PVDF-Cloisite
 200 15A hollow fiber composite membrane, a) cross sectional view (magnification of 150 \times), b)
 201 outer surface (magnification of 15,000 \times) and c) inner surface (magnification of 10,000 \times)

202

203

204

Table 2 Membrane properties and module design

<u>Membrane properties</u>	
Average pore size (nm)	88
Porosity (%)	83.70 ± 0.67
Contact angle ($^{\circ}$)	97.72 ± 2.54
Fiber outer dia. (μm)	763 ± 19
<u>Module design</u>	
Module inner dia. (m)	0.01
Module length (m)	0.22
Number of fibers in module	20
Effective fiber length in module (m)	0.19
Effective membrane area in module (m^2)	0.01

205

206 **2.5 Analytical methods**

207 **2.5.1 Dye and salt concentration determination**

208

209 The dye concentration in the sample solutions was detected by a UV-vis
210 spectrophotometer (DR5000, Hach) which measured at its maximum absorbance wavelength.
211 Meanwhile, the ionic conductivity of the sample solutions was measured using a bench
212 conductivity meter (4520, Jenway). Both sample absorbance and conductivity were later
213 converted into concentration using a calibration curve.

214

215 **2.5.2 SEM-EDX**

216

217 The dry membrane samples were immersed in liquid nitrogen and fractured, followed
218 by sputter-coating with platinum using a sputtering device. The cross-sections of the
219 membrane samples were examined using scanning electron microscope (SEM) (TM-3000,
220 Hitachi). Meanwhile, energy-dispersive X-ray (EDX) spectrometer (XFlash[®] 430H, Bruker)
221 was used for elemental analysis in order to identify the elements caused by foulants that
222 deposited on membrane surface.

223

224 **3 Results and discussion**

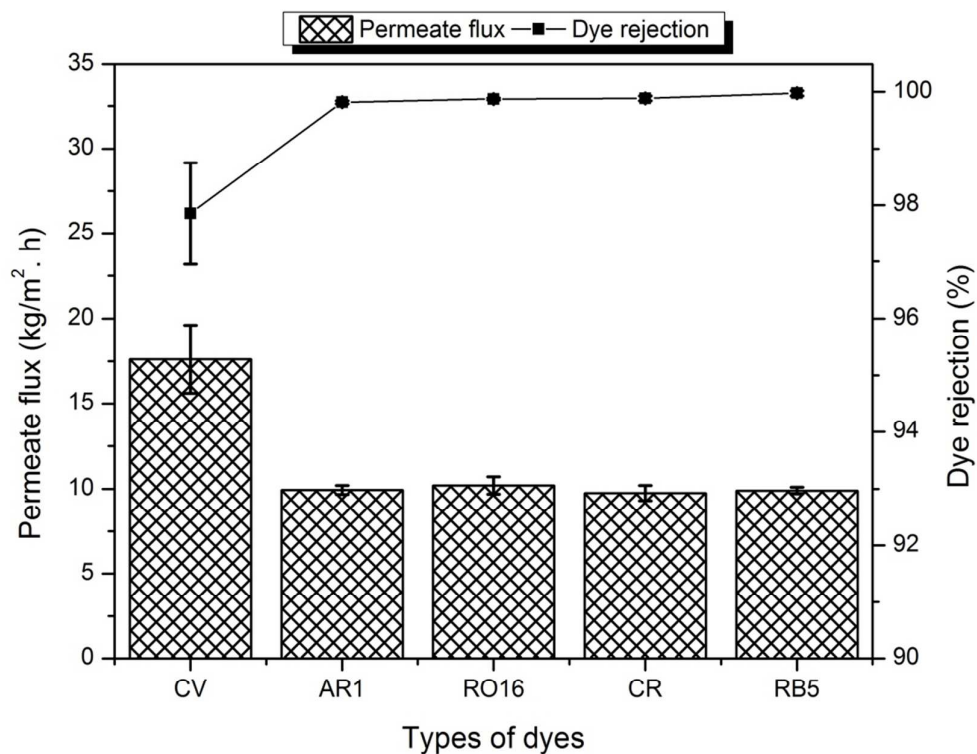
225 **3.1 Effect of dye characteristics on DCMD performance**

226

227 Figure 3 shows the effect of dye characteristics on the permeate flux and rejection of
228 PVDF-Cloisite 15A hollow fiber composite membrane during DCMD process. The error bars
229 indicate the standard deviations of the average measured values of both water flux and dye
230 rejection. From the figure, it can be clearly seen that the in-house made membrane could
231 achieve very similar permeate fluxes (around 10 kg/m².h) for all dyes studied, except for CV
232 which showed >17 kg/m².h. With respect to separation characteristics, it is found that the
233 membrane could potentially eliminate almost all types of dyes regardless of their MW and
234 Stokes diameter. Although the membrane average pore size ($d_p = 88$ nm) is significantly
235 larger than those of dyes' particle size (Table 3), its excellent separation performance is not
236 compromised. This is because MD does not work according to the principle of size exclusion
237 and/or Donnan exclusion as in ultrafiltration and nanofiltration [29–32]. It instead works as a
238 physical barrier to hold the liquid–vapor interface at the entrance of the membrane pores. In

239 view of this, the separation mechanism in MD is predominantly determined by the VLE
 240 principle [33].

241



242

243 **Figure 3** Effect of dye components on the permeate flux and dye rejection of membrane
 244 during DCMD process (Conditions = hot stream: 50 ppm dyeing solution, 70°C at flow rate
 245 of 0.023 m/s; cold stream: distilled water, 20°C at flow rate of 0.010 m/s)

246

247

248

Table 3 Properties of synthetic dyes used in this work

Dye	^a λ_{\max} (nm)	^b MW (g/mol)	^c D_{AB} (10^{-10} m ² /s)	^d d_A (nm)
CV	590	407.98	3.99	1.23
AR1	506	509.42	4.25	1.15
RO16	493	617.54	3.81	1.29
CR	498	696.66	3.24	1.52
RB5	597	991.82	3.01	1.63

249 ^a λ_{\max} = Maximum absorbance wavelength

250 ^bMW = Molecular weight

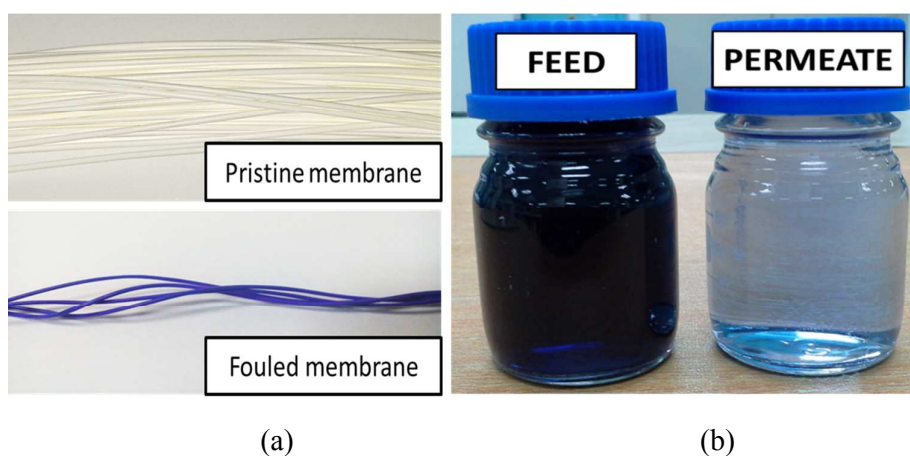
251 ^c D_{AB} = Diffusion coefficient of dye in water

252 ^d d_A = Stokes diameter of dye in water

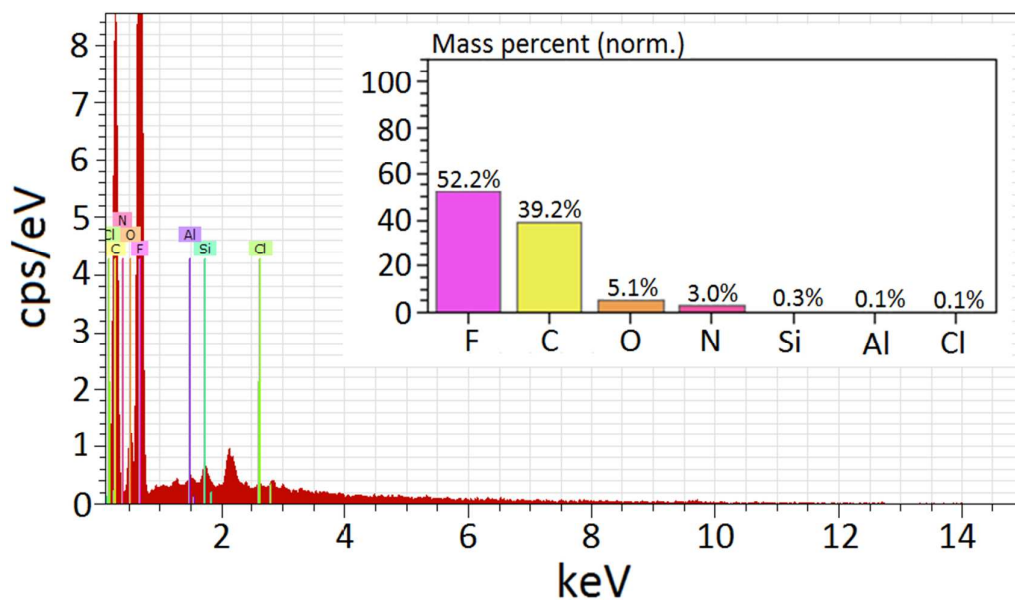
253

254

255 Unlike other dye components which displayed very similar flux and rejection results,
256 the CV dye seemed to have different interaction with the membrane matrix, leading to
257 relatively higher permeate flux but lower removal rate. This can be possibly due to the high
258 “affinity” of this particular dye towards the membrane matrix. The high adsorption rate of
259 CV towards PVDF-based membrane is believed to be the main factor changing the color of
260 membrane after treatment process (see Figure 4(a)). Furthermore, the high diffusivity of CV
261 in aqueous solution could be another reason causing less promising dye removal (<98%) as
262 evidenced from the permeate sample collected (Figure 4(b)). The detection of nitrogen (N)
263 and chlorine (Cl) element on the composite membrane surface as shown in Figure 5 strongly
264 indicates the presence of dye component on the membrane surface, owing to the possible
265 interaction between the aromatic rings of the dye molecule and the membrane via Van der
266 Waals [22].
267



268
269
270 **Figure 4** Direct comparisons between (a) pristine membrane and fouled membrane and (b)
271 50 ppm CV dyeing solution (feed) and permeate produced by the composite membrane
272



273

274

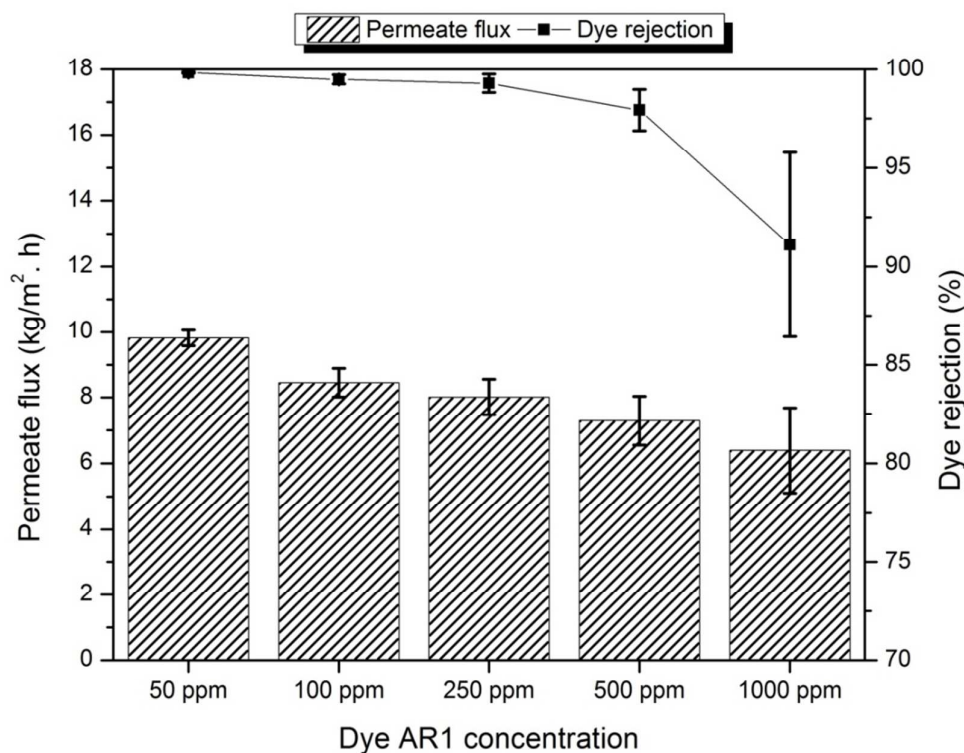
Figure 5 EDX results on the membrane surface after treating CV dyeing solution

275

276 3.2 Effect of dye concentrations on DCMD performance

277

278 In general, approximately 10–20% of textile dyes are lost during dyeing process and
 279 as a consequence, the effluent discharged typically contains between 10 and 1000 ppm of dye
 280 components [34,35]. To evaluate the effect of dye concentration on the DCMD performance,
 281 a series of experiments were carried out and the results are shown in Figure 6. Results
 282 showed that both permeate flux and dye rejection tended to decrease with increasing dye
 283 concentration from 50 to 1000 ppm. The permeate flux decline at high solute concentration
 284 can be caused by the lower water vapor transport rate. This phenomenon is common in MD
 285 process as higher solute concentration could lead to lower activity coefficient of water vapor
 286 pressure [33,36].



287

288 **Figure 6** Permeate flux and dye rejection as a function of dye concentration (Conditions =
289 hot stream: 70°C at flow rate of 0.023 m/s; cold stream: distilled water, 20°C at flow rate of
290 0.010 m/s)

291

292 In addition to activity coefficient of water vapor pressure, the reduction of permeate
293 flux and dye rejection at high concentration of dye solution is also possibly due to the
294 attachment of dye particles on the membrane surface which leads to either partially or fully
295 pore blockage. Additional fouling layer could be developed which further reduces the
296 evaporation area and affects permeate quantity. As reported by Yarlaga *et al.* [37], severe
297 fouling caused by high feed concentration may damage the membrane surface and allow the
298 passage of small quantities of non-volatile solutes through the membrane. In addition,
299 increasing feed concentration will also increase feed viscosity and boundary layer thickness,
300 which enhances the mass transfer resistances [33]. Even though MD experienced lower
301 permeate flux at high dye concentration, its degree of flux decline was still much lower
302 compared to pressure-driven membrane process, e.g. nanofiltration. Comparing the results
303 obtained from lowest and highest dye concentration, it is found that the flux of MD was only
304 reduced by 12.4% with dye rejection maintained at > 90%.

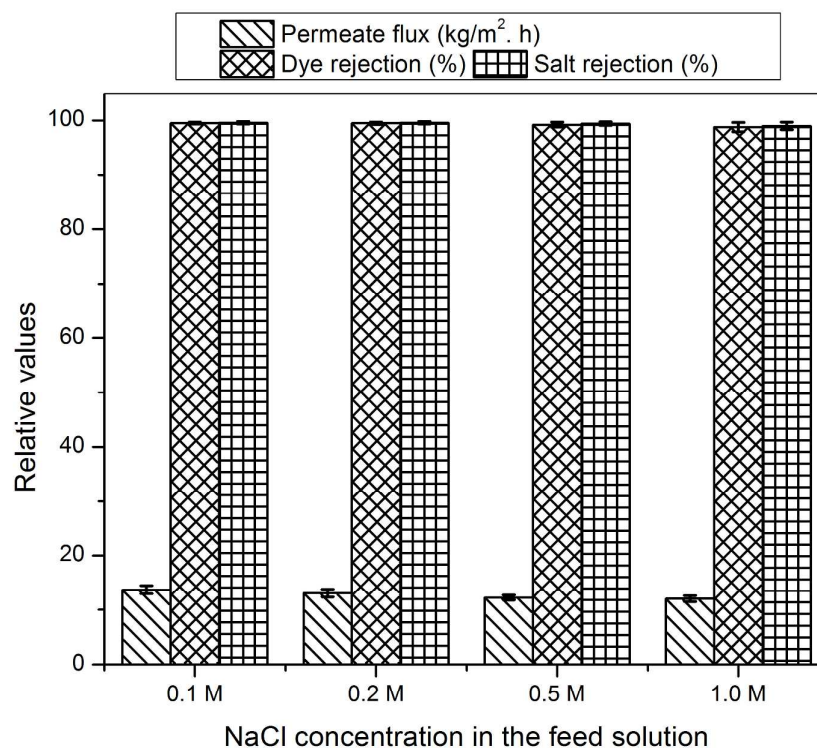
305

306 3.3 Effect of salt concentrations on DCMD performance

307

308 Cotton is the most important and widely used textile fiber in the world which consists
 309 around 88-96% of pure cellulose [38]. However, natural cellulose fibers commonly carry
 310 negative charge, which create repulsion with anionic dyes. In order to promote dye-fiber
 311 fixation, high amount of NaCl is needed to suppress the fiber surface charge. This as a
 312 consequence has led the effluent to have high NaCl concentration (0.7–1.4 M) [39]. In this
 313 section, the effect of feed salt concentration on the performance of DCMD process was
 314 investigated and the results are shown in Figure 7. It can be seen from the figure that the
 315 variation in NaCl concentration in the feed solution has very little impact on the performance
 316 of membrane with respect to permeate flux and separation characteristics. The findings from
 317 this work were consistent with Banat *et al.* [15] in which they also reported that salt
 318 concentration (0.05–1.0 M) has negligible effect on the driving force for the vapor flux.

319

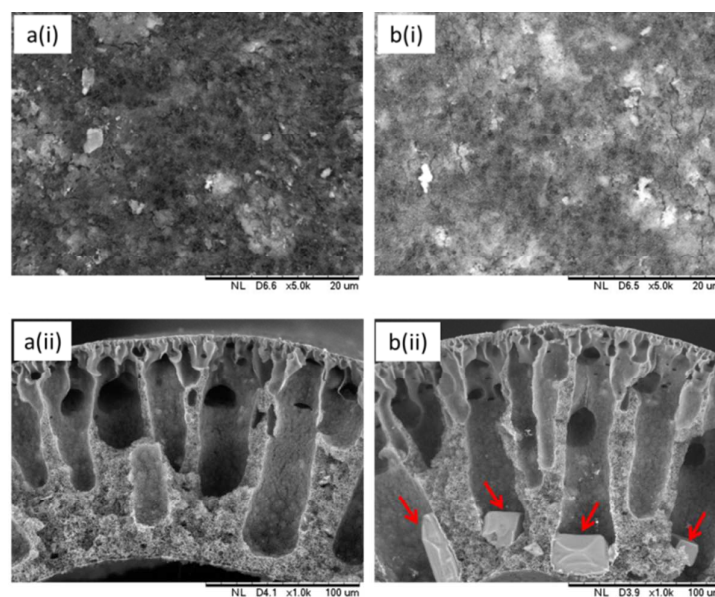


320

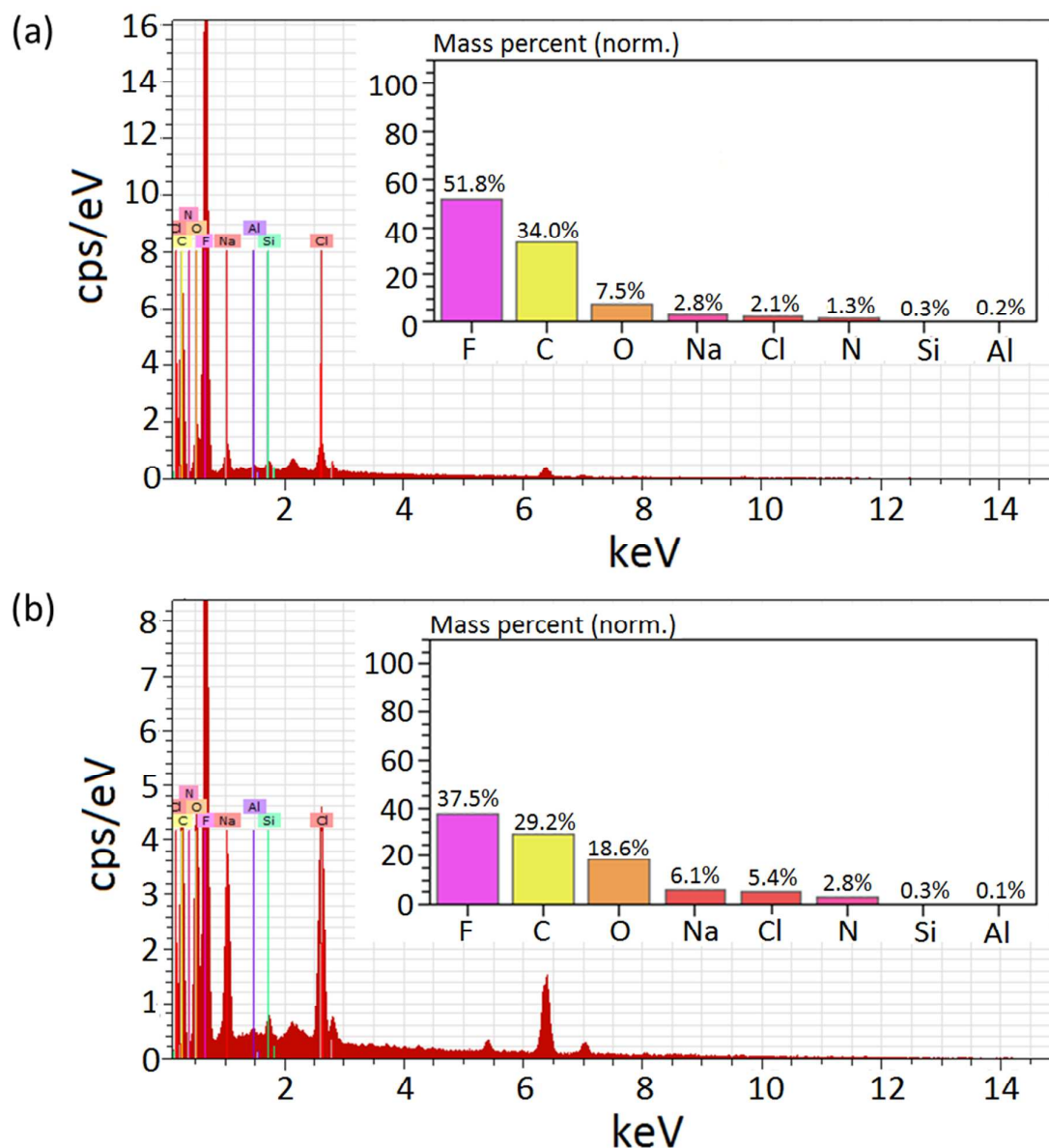
321 **Figure 7** Permeate flux and solute rejection as a function of salt concentration in the dyeing
 322 solution containing 50 ppm ARI (Conditions = hot stream: 70°C at flow rate of 0.023 m/s,
 323 cold stream: 20°C at flow rate of 0.010 m/s)

324

325 Although the salt concentration has negligible effect on membrane permeate flux, it
326 does have huge impact on membrane scaling when it is present at high concentration. Figure
327 8 shows the SEM images of the membranes after testing with two different salt
328 concentrations (0.1 and 1.0 M). Crystallized salts were found within the structure of the
329 fouled membrane after treating 1.0 M NaCl feed solution. This observation could be directly
330 related to membrane scaling [40]. Generally, the scaling occurs when the salt concentration in
331 the feed solution reaches supersaturation due to high product water recovery. Concentration
332 and temperature polarizations are the major causes for the salt solution to become
333 supersaturated and crystallize directly on the membrane surface or crystallize in the bulk
334 solution and deposit on the membrane surface. The presence of salt on the composite
335 membrane was further analysed based on EDX results shown in Figure 9. As can be seen, Na
336 and Cl elements corresponded to salt were detected, in addition to the elements (F, C, O, Si
337 and Al) belonging to the PVDF-Cloisite 15A membrane. Furthermore, the amounts of Na and
338 Cl detected are consistent with the SEM images shown. Since the fouling scaling is
339 hydrophilic, there is a high tendency for the membrane to have pore wetting problems. The
340 membrane scaling however has no obvious influence on the permeate flux because the
341 evaporation area at the feed side did not decrease significantly. In all cases, the solute
342 rejections are still promising, recording >98%. Nevertheless, more research is still needed to
343 examine the long-term effect of crystallized salts (within membrane matrix) on separation
344 performance.



345
346 **Figure 8** SEM images of the i) outer surface and ii) cross-section of the composite membrane
347 after testing with 50 ppm ARI solution containing a) 0.1 M and b) 1.0 M NaCl



348

349 **Figure 9** EDX analysis results of the membranes after testing with different salt
 350 concentrations, a) 0.1 M and b) 1.0 M NaCl

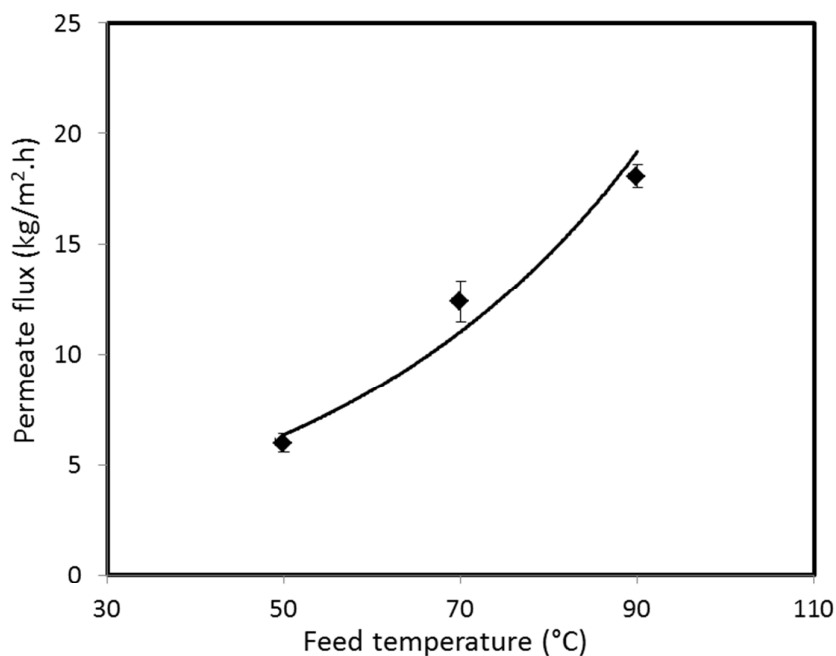
351

352 **3.4 Effect of feed temperature and feed flow rate on DCMD performance**

353

354 Figure 10 shows the effect of feed temperature on the permeate flux of PVDF-Cloisite
 355 15A hollow fiber composite membrane in the feed solution composed of 50 ppm AR1 and 1
 356 M NaCl. As expected, an exponential relation between permeate flux and feed temperature
 357 was observed. This trend could be explained by the Antoine equation which predicts an
 358 exponential relationship between the vapor pressure difference and temperature [15,33]. At

359 low feed temperature, heat is likely to be wasted through conduction across both the
360 membrane material and the gas-filled membrane pores, rather than to be used for water
361 evaporation [41]. However, when the feed temperature is further increased, the latent heat of
362 water evaporation is the main contribution to the total heat transfer which result in
363 significant improvement in permeate flux as evidenced in this work. Although heat loss
364 through conduction still occurs at high feed temperature, the impact can be minimized due to
365 the higher partial vapor pressure at the feed side [42].
366

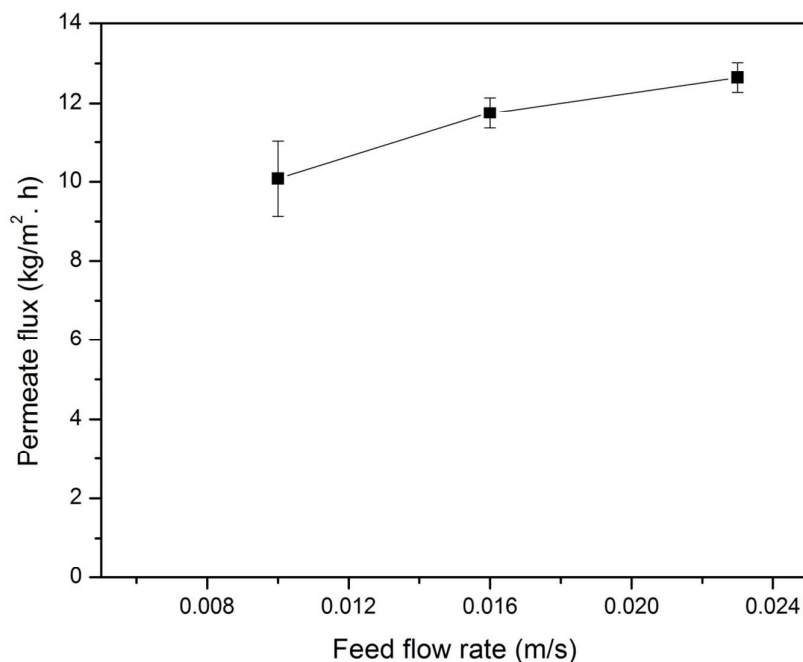


367
368 **Figure 10** Permeate flux as a function of feed temperature (Conditions = hot stream: 50–90°C
369 at flow rate of 0.023 m/s, cold stream: 20°C at flow rate of 0.010 m/s)

370

371 Figure 11 shows the permeate flux of PVDF-Cloisite 15A composite membrane as a
372 function of feed flow rate using feed solution composed of 50 ppm AR1 and 1 M NaCl. It is
373 noticed that the effect of feed flow rate is less significant compared to feed temperature in
374 enhancing permeate flux of membrane. The permeate flux was reported to increase by only
375 25% even though the feed flow rate was greatly increased by more than 100%. The slight
376 enhancement of permeate flux at higher flow rate can be attributed to the decrease in the
377 temperature polarization effect between the membrane surface and the bulk streams [16,43–
378 45]. Although the flux increases with increasing feed flow rate, it is important to ensure that

379 the hydraulic pressure is lower than the wetting pressure while controlling the feed flow rate.
380 This precaution is needed in order to prevent wetting problem during MD process.



381

382 **Figure 11** Permeate flux as a function of feed flow rate (Conditions = hot stream: 70°C at
383 flow rate of 0.010–0.023 m/s, cold stream: 20°C at flow rate of 0.010 m/s)

384

385 3.5 Performance comparison of membrane distillation

386

387 Table 4 compares the performance of the self-made membrane studied in this work
388 with previously published works for the treatment of dyeing solutions. Although other factors
389 such as MD configuration, operating temperatures and feed properties might also affect the
390 MD performance, in addition to the membrane property itself, the results shown in this work
391 have revealed that the performance of the self-made PVDF-Cloisite 15A hollow fiber
392 composite membrane is comparable or even better than the commercial membranes for textile
393 wastewater treatment process. The results proved the in-house made membrane can be a
394 reliable material for the DCMD process, particularly in treating effluents containing dyes and
395 salts. Although VMD in general shows higher flux than DCMD, the objective of using
396 DCMD in this study is due to its relatively simple operation mode and low maintenance cost.
397 For DCMD configuration, both evaporation and condensation processes can occur
398 simultaneously inside the membrane module and it requires no external vacuum pump. Thus,
399 it is more cost-effective to implement.

Table 4 Comparison of the membrane performance obtained in this study with the literature in the MD process for the treatment of dyeing solutions

Membrane material	Membrane configuration	MD configuration	Type of dye (concentration)	J_v (kg/m ² .h)	^a T _f (°C)	^b T _p (°C)	^c R _{color} (%)	References
PP (commercial membrane module)	Hollow fiber	DCMD	Blue E-G (5,000 ppm)	1.62	50	35	100	[46]
PP (Enka Microdyn, USA)	Capillary	VMD	MB (18.5 ppm)	6.3	70	N/A	100	[15]
PP (Membrana GmbH, Germany)	Capillary	VMD	Blue R (50 ppm)	57	60	N/A	> 90	[16]
PP (Membrana GmbH, Germany)	Capillary	Hybrid photocatalysis-DCMD	AR18 (30 ppm)	3.5×10 ⁻³	65	20	100	[17]
PP (Hangzhou Kaijie Membrane Company, China)	Hollow fiber	SPMDR	RB5 (400 ppm)	4.56	65	-	100	[18]
PVDF (fabricated)	Hollow fiber	DCMD	RB5 (50 ppm)	5.64±0.10	80	20	99.83±0.01	[19]
PVDF (fabricated)	Hollow fiber	DCMD	RB5 (500 ppm)	9.82±0.52	60	20	99.86±0.04	[20]
PVDF-Cloisite 15A (fabricated)	Hollow fiber	DCMD	RB5 (50 ppm)	10.13±0.18	70	20	99.98±0.01	[21]
PVDF-Cloisite 15A (fabricated)	Hollow fiber	DCMD	AR1 (50 ppm) and NaCl (1 M)	12.42±0.93	70	20	99.92±0.07	This study

^aT_f= feed temperature, ^bT_p= permeate temperature, ^cR_{color}= color rejection

4 Conclusion

In the present work, the application of DCMD using PVDF-Cloisite 15A hollow fiber composite membrane for dye and salt removal was investigated systematically. Results showed that the in-house made composite membrane demonstrated excellent results in eliminating almost all dye components (except CV dye) with consistent permeate flux recorded irrespective of dye properties. Since CV dye has high affinity towards PVDF-based membrane material and exhibits lowest MW, it can be easily absorbed to membrane matrix, altering membrane color and affecting permeate quality. With respect to dye concentration, it is found that both permeate flux and solute rejection was slightly affected with increasing dye concentration in the feed solution. Reduced permeate flux as a result of increased dye concentration can be attributed to the membrane fouling which increases mass transport resistance. Although salt concentration has no significant effect on membrane performance, the presence of crystallized salts within membrane matrix when the membrane was subject to high concentration of salt solution might need to further analyze, in particular on its effect on membrane long-term performance. In terms of process conditions, it is reported that the increase in both feed temperature and feed flow rate could enhance membrane permeate flux owing to higher latent heat of water evaporation and higher heat transfer coefficient. While this work has focused exclusively on the separation of dyes and salts in aqueous solutions, the effect of surfactants on the activity of the dyes-salts aqueous solution and the performance of membrane is recommended for future work to better examine the potential of MD for industrial wastewater. Besides, effect of solution pH and co-existing ions are also necessary to take into account to better model the textile effluent.

Acknowledgement

The authors gratefully acknowledge Universiti Teknologi Malaysia (UTM) for funding this project under Research University Grant Scheme (Tier 1) (Vot No: Q.J130000.2509.05H48, Title: Separation and Purification of Textile Wastewater using Low-Energy Direct Contact Membrane Distillation (DCMD) Process).

References

- [1] W.J. Lau and A.F. Ismail, Polymeric nanofiltration membranes for textile dye wastewater treatment: Preparation, performance evaluation, transport modelling, and fouling control — a review, *Desalination*, 2009, **245**, 321–348.
- [2] M. Marcucci, I. Ciabatti, A. Matteucci and G. Vernaglione, Membrane technologies applied to textile wastewater treatment, *Ann. N. Y. Acad. Sci.*, 2003, **984**, 53–64.
- [3] R.G. Saratale, G.D. Saratale, J.S. Chang and S.P. Govindwar, Bacterial decolorization and degradation of azo dyes: A review, *J. Taiwan Inst. Chem. Eng.*, 2011, **42**, 138–157.
- [4] B.R. Babu, A.K. Parande, S. Raghu and T.P. Kumar, Cotton Textile Processing: Waste Generation and Effluent Treatment, *J. Cotton Sci.*, 2007, **153**, 141–153.
- [5] A. Ajmal, I. Majeed, R.N. Malik, H. Idriss and M.A. Nadeem, Principles and mechanisms of photocatalytic dye degradation on TiO₂ based photocatalysts: a comparative overview, *RSC Adv.*, 2014, **4**, 37003–37026.
- [6] S. Sen and G.N. Demirer, Anaerobic Treatment of Synthetic Textile Wastewater Containing a Reactive Azo Dye, *J. Environ. Eng.*, 2003, **129**, 595–601.
- [7] M. Lucas and J. Peres, Decolorization of the azo dye Reactive Black 5 by Fenton and photo-Fenton oxidation, *Dyes Pigments*, 2006, **71**, 236–244.
- [8] S. Thomas, R. Sreekanth, V.A. Sijumon, U.K. Aravind and C.T. Aravindakumar, Oxidative degradation of Acid Red 1 in aqueous medium, *Chem. Eng. J.*, 2014, **244**, 473–482.
- [9] G. Crini, Kinetic and equilibrium studies on the removal of cationic dyes from aqueous solution by adsorption onto a cyclodextrin polymer, *Dyes Pigments*, 2008, **77**, 415–426.
- [10] N. Ravindran and G. Balasubramani, Role of White Rot Fungi in Textile Dye Degradation, *Int. J. Adv. Interdiscip. Res.*, 2014, **1**, 38–44.
- [11] J. Chen, Q. Wang, Z. Hua and G. Du, Research and application of biotechnology in textile industries in China, *Enzyme Microb. Technol.*, 2007, **40**, 1651–1655.
- [12] M. Chhabra, S. Mishra and T.R. Sreekrishnan, Combination of chemical and enzymatic treatment for efficient decolorization/degradation of textile effluent: High operational stability of the continuous process, *Biochem. Eng. J.*, 2015, **93**, 17–24.

- [13] N. Tüfekci, N. Sivri and İ. Toroz, Pollutants of Textile Industry Wastewater and Assessment of its Discharge Limits by Water Quality Standards, *Turkish J. Fish. Aquat. Sci.*, 2007, **7**, 97–103.
- [14] J. Dasgupta, J. Sikder, S. Chakraborty, S. Curcio and E. Drioli, Remediation of textile effluents by membrane based treatment techniques: A state of the art review, *J. Environ. Manage.*, 2015, **147**, 55–72.
- [15] F. Banat, S. Al-Asheh and M. Qtaishat, Treatment of waters colored with methylene blue dye by vacuum membrane distillation, *Desalination*, 2005, **174**, 87–96.
- [16] A. Criscuoli, J. Zhong, A. Figoli, M.C. Carnevale, R. Huang and E. Drioli, Treatment of dye solutions by vacuum membrane distillation, *Water Res.*, 2008, **42**, 5031–5037.
- [17] S. Mozia, A.W. Morawski, M. Toyoda and T. Tsumura, Integration of photocatalysis and membrane distillation for removal of mono- and poly-azo dyes from water, *Desalination*, 2010, **250**, 666–672.
- [18] D. Qu, Z. Qiang, S. Xiao, Q. Liu, Y. Lei and T. Zhou, Degradation of Reactive Black 5 in a submerged photocatalytic membrane distillation reactor with microwave electrodeless lamps as light source, *Sep. Purif. Technol.*, 2014, **122**, 54–59.
- [19] N.M. Mokhtar, W.J. Lau and A.F. Ismail, The potential of membrane distillation in recovering water from hot dyeing solution, *J. Water Process Eng.*, 2014, **2**, 71–78.
- [20] N.M. Mokhtar, W.J. Lau, B.C. Ng, A.F. Ismail and D. Veerasamy, Preparation and characterization of PVDF membranes incorporated with different additives for dyeing solution treatment using membrane distillation, *Desalin. Water Treat.*, 2014; DOI:10.1080/19443994.2014.959063.
- [21] N.M. Mokhtar, W.J. Lau, A.F. Ismail and B.C. Ng, Physicochemical study of polyvinylidene fluoride-Cloisite15A[®] composite membranes for membrane distillation application, *RSC Adv.*, 2014, **4**, 63367–63379.
- [22] N.M. Mokhtar, W.J. Lau and A.F. Ismail, Dye wastewater treatment by direct contact membrane distillation using polyvinylidene fluoride hollow fiber membranes, *J. Polym. Eng.*, (2014). DOI: 10.1515/polyeng-2014-0214.
- [23] P.J. Lin, M.C. Yang, Y.L. Li and J.H. Chen, Prevention of surfactant wetting with agarose hydrogel layer for direct contact membrane distillation used in dyeing wastewater treatment, *J. Membr. Sci.*, 2014, **475**, 511–520.
- [24] M.S. El-Bourawi, Z. Ding, R. Ma and M. Khayet, A framework for better understanding membrane distillation separation process, *J. Membr. Sci.*, 2006, **285**, 4–29.

- [25] K.W. Lawson and D.R. Lloyd, Membrane distillation, *J. Membr. Sci.*, 1997, **124**, 1–25.
- [26] K. Hunger, *Industrial Dyes*, Wiley-VCH Verlag GmbH & Co. Germany, 2002.
- [27] N.A.A. Sani, W.J. Lau and A. F. Ismail, Influence of polymer concentration in casting solution and solvent-solute-membrane interactions on performance of polyphenylsulfone (PPSU) nanofiltration membrane in alcohol solvents, *J. Polym. Eng.*, 2014, **34**, 489–500.
- [28] S. Darvishmanesh, J. Vanneste, E. Tocci, J. Jansen, F. Tasseli, J. Degreve, E. Drioli and B. Van der Bruggen, Physicochemical Characterization of Solute Retention in Solvent Resistant Nanofiltration: the effect of solute size, polarity, dipole moment, and solubility parameter, *J. Phys. Chem. B.*, 2011, **115**, 14507–14517.
- [29] E. Alventosa-deLara, S. Barredo-Damas, E. Zuriaga-Agustí, M.I. Alcaina-Miranda and M.I. Iborra-Clar, Ultrafiltration ceramic membrane performance during the treatment of model solutions containing dye and salt, *Sep. Purif. Technol.*, 2014, **129**, 96–105.
- [30] E. Zuriaga-Agustí, E. Alventosa-deLara, S. Barredo-Damas, M.I. Alcaina-Miranda, M.I. Iborra-Clar and J.A. Mendoza-Roca, Performance of ceramic ultrafiltration membranes and fouling behavior of a dye-polysaccharide binary system, *Water Res.*, 2014, **54**, 199–210.
- [31] A.F. Ismail and W.J. Lau, Influence of feed conditions on the rejection of salt and dye in aqueous solution by different characteristics of hollow fiber nanofiltration membranes, *Desalin. Water Treat.*, 2009, **6**, 281–288.
- [32] X. Wei, X. Kong, C. Sun and J. Chen, Characterization and application of a thin-film composite nanofiltration hollow fiber membrane for dye desalination and concentration, *Chem. Eng. J.*, 2013, **223**, 172–182.
- [33] M. Khayet and T. Matsuura, *Membrane Distillation: Principles and Applications*, Elsevier Science, Amsterdam, 2011.
- [34] P. Gharbani, S.M. Tabatabaie and A. Mehrizad, Removal of Congo red from textile wastewater by ozonation, *Int. J. Environ. Sci. Technol.*, 2008, **5**, 495–500.
- [35] N.H. Ince and G. Tezcanh, Treatability of textile dye-bath effluents by advanced oxidation: preparation for reuse, *Water Sci. Tech.*, 1999, **40**, 183–190.
- [36] H. Liu and J. Wang, Treatment of radioactive wastewater using direct contact membrane distillation, *J. Hazard. Mater.*, 2013, **261**, 307–315.

- [37] S. Yarlagadda, V.G. Gude, L.M. Camacho, S. Pinappu and S. Deng, Potable water recovery from As, U, and F contaminated ground waters by direct contact membrane distillation process, *J. Hazard. Mater.*, 2011, **192**, 1388–1394.
- [38] A.M. Gamal, S.A.A. Farha, H.B. Sallam, G.E.A. Mahmoud and L.F.M. Ismail, Kinetic Study and Equilibrium Isotherm Analysis of Reactive Dyes Adsorption onto Cotton Fiber, *Nature and Science*, 2010, **8**, 95–110.
- [39] L. Ji, Y. Zhang, E. Liu, Y. Zhang and C. Xiao, Separation behavior of NF membrane for dye/salt mixtures, *Desalin. Water Treat.*, 2013, **51**, 3721–3727.
- [40] M. Gryta, Alkaline scaling in the membrane distillation process, *Desalination*, 2008, **228**, 128–134.
- [41] K.Y. Wang, S.W. Foo and T.S. Chung, Mixed Matrix PVDF Hollow Fiber Membranes with Nanoscale Pores for Desalination through Direct Contact Membrane Distillation, *Ind. Eng. Chem. Res.*, 2009, **48**, 4474–4483.
- [42] H. Susanto, Towards practical implementations of membrane distillation, *Chem. Eng Process: Process Intensif.*, 2011, **50**, 139–150.
- [43] S. Bonyadi and T.S. Chung, Highly porous and macrovoid-free PVDF hollow fiber membranes for membrane distillation by a solvent-dope solution co-extrusion approach, *J. Membr. Sci.*, 2009, **331**, 66–74.
- [44] T.C. Chen, C.D. Ho and H.M. Yeh, Theoretical modeling and experimental analysis of direct contact membrane distillation, *J. Membr. Sci.*, 2009, **330**, 279–287.
- [45] V. Calabro, E. Drioli and F. Matera, Membrane distillation in the textile wastewater treatment, *Desalination*, 1991, **83**, 209–224.